Optical anisotropy in InAs/AlSb superlattices

Paulo V. Santos, P. Etchegoin, and M. Cardona,
Max-Planck-Institut für Festkörperforschung, Heisenbergstrasse 1, D-70569 Stuttgart, Federal Republic of Germany

B. Brar and H. Kroemer
Department of Electrical and Computer Engineering University of California, Santa Barbara, California 93106
(Received 16 March 1994)

The optical anisotropy in the layer plane of (100) InAs/AlSb superlattices was investigated by ellipsometry and by reflection difference spectroscopy. The superlattices are anisotropic in the (100) plane with the dielectric function along the [011] and [01$\bar{1}$] axes differing by as much as $\sim 5\%$ in the energy range from 2 to 4 eV. The anisotropy in superlattices with either only AlAs or only InSb interface bonds is attributed to a reduction of the D_{2d} symmetry of a perfect structure due to differences between the interfaces where InAs is grown on AlSb and those where AlSb is deposited on InAs. Different mechanisms for the interface-related anisotropy are discussed.

I. INTRODUCTION

Superlattices of III-V zinc-blende semiconductors grown along the [100] direction, such as GaAs/AlAs structures, are normally optically uniaxial with the optical axis along the growth direction. The optical properties of these structures should, therefore, be isotropic in the layer plane. Recently, however, there has been increasing evidence for anisotropic effects in the in-layer excitonic properties of these structures.[1–4] The observed anisotropy, which must arise from a reduction of the D_{2d} point-group symmetry of ideal structures, has been attributed to differences between the top and bottom interfaces of each layer.[1,3] These differences are probably related to the growth process, which may yield different material intermixing, step density and orientation, and local stress for the two kinds of interfaces.

In this paper we investigate optical anisotropy in (100) InAs/AlSb superlattices. These structures combine the large electron mobility of InAs with a large electron confinement energy (above 1 eV) in the InAs wells and have, therefore, potential applications in high-speed electronic devices. Since both the anions and the cations are changed at the interfaces, these superlattices can be grown with interfaces containing ideally either only InSb, only AlAs bonds, or any combination of alternating InSb and AlAs bonds.[5] As will be discussed in detail below, the point-group symmetry of the superlattices depends on the interface type, making them ideal for the investigation of interface effects on the in-plane optical anisotropy. Superlattices with alternating InSb and AlAs bonds exhibit C_{2v} point-group symmetry: these structures are anisotropic in the layer plane with optical axes in the [011] and [01$\bar{1}$] directions. Structures with a single type of interface bond (i.e., either only InSb or only AlAs bonds), on the other hand, possess D_{2d} point-group symmetry and should ideally be optically isotropic in the plane of the superlattice layers. Deviation from ideality gives rise to an anisotropy in the optical properties, so that the degree of anisotropy is a measure of interface quality.

The optical anisotropy in the superlattices was investigated by spectroscopic ellipsometry and by reflection difference spectroscopy (RDS) for photon energies between 1.5 and 5.5 eV. RDS is particularly sensitive to small (i.e., in the $< 0.1\%$ range) differences in the optical properties and has been successfully used in the last years to probe surface-induced optical anisotropies in semiconductors.[15] We observed optical anisotropy not only in structures with alternating AlAs and InSb interface bonds, but also in those with nominally only InSb or only AlAs interfaces. The reflectance anisotropy in the latter case is attributed to a reduction of the ideal D_{2d} symmetry due to differences between the interfaces where InAs is grown on AlSb and those where AlSb is deposited on InAs. Differences between the top and the bottom interfaces of the InAs layers in InAs/AlSb superlattices with AlAs interface bonds have been previously detected in transport measurements.[5] The present study indicates that interface asymmetry is a more fundamental property of the superlattices and is also present in structures with nominally only InSb interface bonds. Different mechanisms for the anisotropy are discussed and compared to the experimental data.

II. EXPERIMENT

The InAs/AlSb superlattices used in this study were grown on an AlSb buffer layer deposited on the (100) face of semi-insulating GaAs substrates by molecular beam epitaxy. The samples were terminated with an InAs capping layer to prevent oxidation of the AlSb films. Further details of the deposition process can be found in Ref. 5 and a structural characterization of the superlattices is presented in Refs. 6–8 and 15. Results will be presented for samples with six bilayers (one bilayer= $a/2$, where a is the lattice constant) of InAs and six bilayers

0163-1829/94/50(12)/8746(9)/$06.00

of AlSb per superlattice period. All samples were grown under similar conditions except for the interfacial composition. We also investigated a second set of samples with a larger period (nine bilayers of InAs and AlSb per period). No qualitative differences were found between the optical properties of the two sets.

As mentioned above, the structures can thus be grown with interfaces containing either only AlAs interface bonds (AlAs type), only InSb interface bonds (InSb type), or both kinds of bonds simultaneously. The atomic structure for superlattices with different kinds of interfaces, projected on the $(01\bar{1})$ plane is illustrated in Fig. 1. The covalent bonds between a cation and an overlaying anion, represented by the tilted lines connecting the atoms, are either in the [111] or in the $[1\bar{1}\bar{1}]$ direction. The bonds between an anion and an overlaying cation, on the other hand, are in the $[11\bar{1}]$ and $[1\bar{1}1]$ directions (horizontal lines). The interface bonds are represented by double lines in Fig. 1. For superlattices with AlAs-like (InSb-like) interfaces the InAs layers are terminated with As (In) atoms and the AlSb layers with Al (Sb) atoms. Control of interface composition is achieved by exposing each interface to an As (Sb in the case of InSb interfaces) prior to the deposition of the successive layer.[5] Note that each superlattice period contains six planes of In and six planes of Al atoms. However, depending on the nature of the interface, the number of planes of column VI elements (Sb of As) can be 5, 6, or 7.

It is easy to see from Fig. 1 that the superlattices with a single type of interface bond (i.e., AlAs-like of InSb-like interfaces) have mirror reflection planes with normals along the [011] and $[01\bar{1}]$ directions. They also have a fourfold improper rotation axis (S_4) around the [100] direction (point group D_{2d}). Their optical axis is along the growth direction and the dielectric function is isotropic for polarizations in the layer plane. Structures with alternating InSb- and AlAs-like interfaces belong to point group C_{2v} (no S_4 axis) and have three dielectric axes: one along the growth direction ([100] direction) and the other two along [011] and $[01\bar{1}]$. These superlattices are, therefore, birefringent in the layer plane.

We have investigated the linear optical response of InAs/AlSb superlattices using ellipsometry and reflectance difference spectroscopy. The ellipsometry measurements were performed with plane of incidence both parallel and perpendicular to the [011] direction. The ellipsometric angles were converted into the pseudodielectric function using a two-phase model composed of a sharp interface between the sample and air. RDS measures the relative difference $\frac{r_a - r_b}{\bar{r}} = 2(r_a - r_b)/(r_a + r_b)$ between the complex reflection coefficient r along two perpendicular directions **a** and **b** along the sample surface. The real and imaginary parts of the RDS signal ($= \frac{r_a - r_b}{\bar{r}}$) are related, respectively, to the relative difference in the reflection coefficient, R (i.e., $\frac{r_a - r_b}{\bar{r}} = \frac{1}{2}\frac{R_a - R_b}{\bar{R}}$) and to the difference in the phase change upon reflection Δ for incident polarizations along the **a** and the **b** directions.[9-11] In the RDS measurements linearly polarized light along the **a** + **b** direction was impinged on the sample surface at quasinormal incidence (incidence angle $< 10°$) and the polarization of the reflected light was analyzed using an acousto-optical modulator. Details of the experimental RDS setup are described in Refs. 10 and 11. As a differential technique, RDS can detect small anisotropies in the complex reflection coefficient since the isotropic contribution is eliminated. All experiments were performed in air and at room temperature.

III. RESULTS

Figure 2 shows raw RDS spectra of InAs/AlSb superlattices with AlAs interface bonds. The samples consist of 138 double layers of InAs and AlSb, each six bilayers thick. The thin lines were obtained for incident light polarized in the $[\bar{0}11]$ direction and correspond to the real and imaginary parts of $\frac{r_{[010]} - r_{[001]}}{\bar{r}}$. The spec-

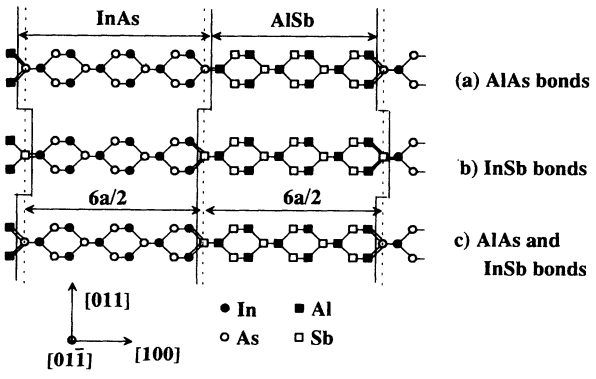

FIG. 1. Atomic configuration projected in the plane perpendicular to the $[01\bar{1}]$ direction for InAs/AlSb superlattice with (a) AlAs-like, (b) InSb-like, and (c) both AlAs-like and InSb-like interfaces. The interface bonds are represented by the double bonds and the interface position is indicated by the vertical solid lines.

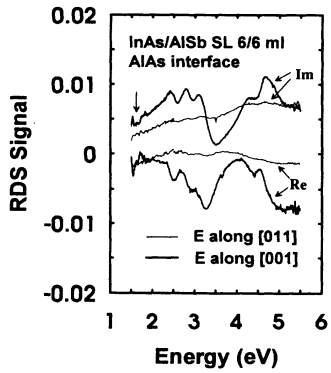

FIG. 2. Relative difference in the complex reflectivity (RDS signal $= \frac{r_a - r_b}{\bar{r}}$) between the **a** = [010] and **b** = [001] directions (thin lines) and between the **a** = [011] and **b** = $[01\bar{1}]$ directions (thick lines) for InAs/AlSb superlattices with AlAs-like interface bonds.

tra show weak features, which are probably due to small sample misalignment and to the finite angle of incidence of the incoming light. The background linear increase in $\mathrm{Im}\left(\frac{r_{[010]}-r_{[001]}}{\bar{r}}\right)$ with energy is an artifact of the measuring technique associated with the optical activity of the optical components. The optical response is, therefore, essentially identical in the [011] and in the [01$\bar{1}$] directions, a fact which singles out these directions as the dielectric axes.

The second set of data in Fig. 2 (thick lines) were obtained after rotating the sample by 45° around the growth axis so as to put the incident polarization in the [001] direction. The RDS signal in this case is proportional to the difference in reflectivity for incident fields in the [011] and [01$\bar{1}$] directions. Contrary to the expectation for samples with a single kind of interface bond, the RDS signal shows differences of the order of 2% between the reflectivity in those two directions.

The structures in the RDS spectra depend on the kind of interface bonds present in the sample. Figure 3 displays the real part of the RDS signal for samples with different kinds of interfaces between an AlSb layer and an overlaying InAs layer (hereafter denoted as the bottom interfaces of the InAs wells) and between an InAs layer and an overlaying AlSb film (top interfaces). In order to correct for the optical activity and for small misalignments of the optical components the data presented in Fig. 3 correspond to the difference $\frac{r_{[011]}-r_{[01\bar{1}]}}{\bar{r}} - \frac{r_{[010]}-r_{[001]}}{\bar{r}}$ between the RDS data obtained with incident fields in the [001] and the [011] directions. All samples in Fig. 3 have six bilayer-thick InAs and AlSb layers.

Figures 3(a) and 3(d) are for samples with only InSb and only AlAs interfaces, respectively. In the first case the RDS spectrum [Fig. 3(a)] is dominated by a minimum in $\mathrm{Re}\frac{r_{[011]}-r_{[01\bar{1}]}}{\bar{r}}$ at 2.8 eV. For samples with AlAs interface bonds, the minimum is shifted to 3.3 eV [Fig. 3(d)]. Figures 3(b) and 3(c) are for superlattices containing both types of interface bonds. These structures are thinner than those in Figs. 3(a) and 3(d) and partially transparent below 2 eV. The oscillations in this energy range result from Fabry-Perot interference in the total thickness of the superlattice film. It is interesting to note that although these structures are inherently anisotropic, the magnitude of the anisotropy is comparable to that found in superlattices with a single type of interface bonds [note, however, that Fig. 3(c) exhibits the largest anisotropy of the four samples under consideration]. In addition, the spectral shape changes when the bond types of the bottom and top interfaces of the InAs layers are interchanged [Figs. 3(b) and 3(c)], indicating that the interface properties depend on the deposition order of the superlattice layers.

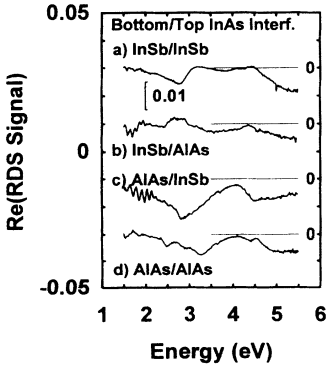

FIG. 3. Real part of RDS signal ($\frac{r_{[011]}-r_{[01\bar{1}]}}{\bar{r}}$) for InAs/AlSb superlattices with different bottom and top interfaces for the InAs layers. In the notation A/B, A and B correspond to the bond type present in the bottom and top interfaces of the InAs layers, respectively. The spectra are shifted vertically for clarity and the horizontal lines indicate the reference (zero) position in each case.

The changes in the RDS spectra with interface bonding type indicate that the optical anisotropy must be related to the interface composition. RDS data can be used to determine the difference in the dielectric constant $\Delta\epsilon = \epsilon_{[011]} - \epsilon_{[01\bar{1}]}$ between the [011] and [01$\bar{1}$] directions. For that purpose, the superlattices were treated as a uniaxial medium with an optical axis in the [011] direction. For small anisotropies between two perpendicular directions **a** and **b**, the complex reflectivity and the dielectric constants are related by[15]

$$\frac{\Delta\epsilon}{\bar{\epsilon}} = \frac{\epsilon_{\mathbf{a}} - \epsilon_{\mathbf{b}}}{\bar{\epsilon}} = \frac{(\bar{\epsilon}-1)}{\sqrt{\bar{\epsilon}}}\frac{r_{\mathbf{a}} - r_{\mathbf{b}}}{\bar{r}}, \tag{1}$$

where $\bar{\epsilon} = (\epsilon_{\mathbf{a}} + \epsilon_{\mathbf{b}})/2$.

The anisotropy in the dielectric constant $\epsilon_{[011]} - \epsilon_{[01\bar{1}]}$ obtained from Eq. 1 is shown by the thick lines in Figs. 4(a) and 4(b) for superlattices with AlAs-like and InSb-like interfaces, respectively. The dielectric constant $\epsilon_{[110]}$ necessary for the calculation was determined by spectroscopic ellipsometry.

The real and imaginary parts of $\epsilon_{[011]}$ and $\epsilon_{[01\bar{1}]}$ differ by approximately 0.6 to 0.8 units between 2.5 and 3 eV, as compared to the absolute values of approximately 15 for the real and imaginary parts in the same energy range. Most of the structures in $\epsilon_{[011]} - \epsilon_{[01\bar{1}]}$ for the sample with AlAs interface bonds correspond closely to those observed in the dielectric constant of bulk InAs and bulk AlSb. The position of these critical points for bulk InAs (AlSb) is indicated by the solid (dot-dashed) vertical lines in Fig. 4.[12–14] The onset of the anisotropy in the imaginary part of $\epsilon_{[011]} - \epsilon_{[01\bar{1}]}$ at 2.4 eV coincides with the critical point E_1(InAs).[12] The main feature in $\mathrm{Im}(\epsilon_{[011]} - \epsilon_{[01\bar{1}]})$ in Fig. 4a is located at 3.2 eV, close to $(E_1 + \Delta_1)$(AlSb). The shoulder at 2.95 eV in the same spectrum is only ~ 0.1 eV above E_1(AlSb). Finally, the features in $\mathrm{Im}(\epsilon_{[011]} - \epsilon_{[01\bar{1}]})$ between 4 and 5 eV lay near the critical points E_2 of InAs and AlSb.

In the superlattice with InSb interface bonds [Fig. 4(b)] the energies of the main features in $\mathrm{Im}(\epsilon_{[011]} - \epsilon_{[01\bar{1}]})$ correspond to E_1(InAs) (shoulder at 2.5 eV) and $(E_1 + \Delta_1)$(InAs) (or possibly also E_1(AlSb)) at 2.8 eV. The main difference to the previous case is that the contribution from critical points of the AlSb layers [especially $(E_1 + \Delta_1)$(AlSb), which is the dominant fea-

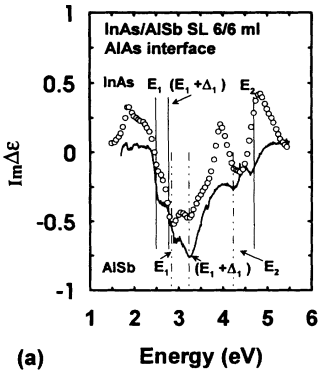

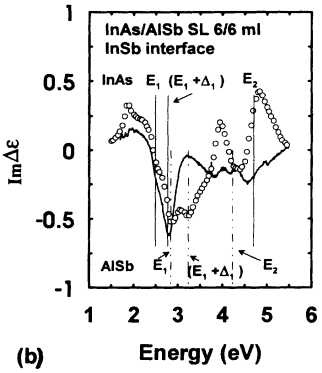

FIG. 4. Imaginary part of the difference between the dielectric function in the [011] and in the [01$\bar{1}$] directions, $\Delta\epsilon = \epsilon_{[011]} - \epsilon_{[01\bar{1}]}$, for InAs/AlSb superlattices with (a) AlAs-like and (b) InSb-like interfaces. The circles indicate the disorder contribution to the anisotropy estimated from the bond polarizability model (see text for details). The vertical solid and dot-dashed lines indicate the energy position of the critical points for bulk InAs and AlSb, respectively.

ture in Fig. 4(a)], has a different sign from that from the InAs layers. These differences will be discussed in the following sections.

IV. DISCUSSION

The anisotropy observed in superlattices with either only AlAs or only InSb interface bonds arises from a breakdown of the selection rule for the optical transitions expected for the D_{2d} point group of these superlattices. Optical anisotropies have been previously observed both in bulk III-V materials and superlattices. In the case of bulk semiconductors,[15–17] the anisotropy has been attributed to the loss of perfect periodicity induced by the presence of the surface. The amplitude of the anisotropy in the reflection coefficient (i.e., $\frac{R_{[011]}-R_{[01\bar{1}]}}{\bar{R}}$) depends on the crystal surface and, above the fundamental gap, is smaller $< 0.5\%$ for the (100) GaAs surface.[15,17] These anisotropies are significantly smaller than the $\sim 1.5\%$ to 2% anisotropies observed in Fig. 2. For (100) surfaces the main contribution to the anisotropy has been identified as a surface many-body effect arising from the reduced local field effects for the atoms near the surface due to the termination of the bulk lattice.[15,17,18] The difficulty in applying this mechanism to the InAs/AlSb superlattices resides in the fact that the main contribution to the anisotropy in bulk samples arises from the first two to four atomic planes near the surface. The RDS spectra should, therefore, be dominated by the contribution from the InAs layer and show only weak structures from AlSb, in contradiction with the results of Fig. 4. This mechanism cannot, therefore, account for the main features in the RDS spectra of the superlattice, at least for energies below ~ 4 eV. It can, however, be important for higher energies where light absorption takes place mainly in the top InAs layer.

In-plane anisotropies have also been observed in the excitonic spectra of GaAs/AlAs superlattices,[1,2] where it has been attributed to differences between the top and lower interfaces of a single layer. The interface asymmetry may arise from differences in composition, roughness amplitude and orientation,[19,20] and localized strains[2] for the two interfaces. The dependence of the RDS spectra of InAs/AlSb superlattices on interface composition strongly suggests that a similar mechanism may account for the optical anisotropy, i.e., the interfaces where InAs is deposited on AlSb (the bottom interface of the InAs wells) must be different from those where AlSb is grown on InAs (top interface of the InAs wells). The existence of an interface asymmetry was inferred from the transport properties of AlSb/InAs/AlSb quantum wells with different types of interface bonds by Tuttle and co-workers.[5] These authors verified that the presence of AlAs bonds in the bottom interfaces of the InAs wells considerably degrades the electronic mobility in the wells whereas the degradation is less extensive or even absent when these bonds are only at the top interface. The asymmetry may arise, for instance, from differences in the composition of the interfacial bilayer (AlAs and InSb, for superlattices with AlAs and InSb interface bonds, respectively) in the two interfaces due to intermixing of cations or anions. Note that a symmetric broadening of the composition profile at the interfaces as a consequence, for instance, of material interdiffusion does not change the symmetry properties of the superlattice and cannot, therefore, account for the anisotropy in the layer plane. In fact, we are going to see that a disorder-induced anisotropy is mainly determined by the interface composition and is not sensitive to the amount of interdiffusion into the adjoining layer.

In the following, we discuss different mechanisms for the interface-induced anisotropy in the InAs/AlSb superlattices. Most of the discussion will be restricted to superlattices with a single type of interface bonds. First, we estimate the anisotropy in periodic structures with different kinds of interfaces using microscopic tight-binding calculations of the optical properties of the superlattices. The main anisotropy mechanism in this case is the reduction in the symmetry of the superlattice layers induced by asymmetric interfaces. The second mechanism describes the effects of interface disorder on the optical properties in the framework of the bond polarizability model. The

bonds are assumed to have different polarizabilities for polarizations along and perpendicular to the bond direction and the anisotropy arises from differences in densities and type of bonds contributing to polarization along the [011] and [01$\bar{1}$] directions. Since the anisotropy in this case is a sum of incoherent individual contributions, this mechanism is applicable if long-range correlations are destroyed by chemical disorder in the superlattice layers. As we shall see, the contribution to the anisotropy comes from bonds near the interfaces and is, therefore, very sensitive to the interface composition and degree of disorder. The disorder mechanism predicts contributions of the same sign for the InAs and for the AlSb critical points, and describes relatively well the anisotropy in superlattices with AlAs interface bonds.

The third mechanism describes the effects of interface roughness on the anisotropy. We will assume that the roughness arises from variations of the layer thickness along the sample surface. In order to yield an anisotropic contribution, the thickness variations must have a preferential orientation along the sample surface. This mechanism seems to yield the main contribution for the anisotropy in superlattices with InSb interface layers.

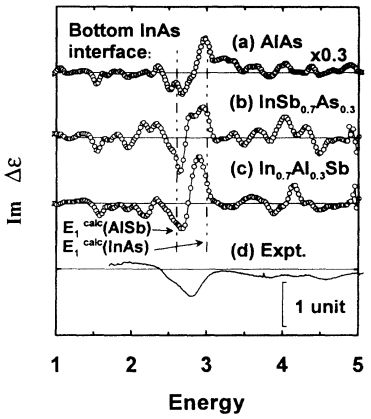

FIG. 5. Imaginary part of $\Delta\epsilon = \epsilon_{[011]} - \epsilon_{[01\bar{1}]}$ calculated from an empirical tight-binding band structure calculation for InAs/InSb superlattice. The bottom interface of the InAs layers is composed of InSb bond and the top interface consists of (a) AlAs bonds, (b) InSb bonds with 30% of the Sb atoms replaced by As, and (c) InSb bonds with 30% of the In atoms replaced by Al. Curve (d) reproduces the anisotropy measured in superlattices containing nominally only InSb interface bonds. The vertical dot-dashed lines indicate the location of the critical points $E_1^{\rm calc}$(InAs) and $E_1^{\rm calc}$(InAs) obtained from tight-binding calculations of the dielectric function of the corresponding bulk materials.

A. Microscopic calculations

In order to determine the effects of the interface on the optical properties, we performed microscopic calculations of the superlattice dielectric constant using the empirical tight-binding method. The calculations used a basis consisting of 5 sp^3s^* orbitals[21] and did not include spin-orbit coupling. The matrix elements for the tight-binding Hamiltonian of InAs and AlSb were extracted from Ref. 18. The valence band offset between InAs and AlSb was added to the intra-atomic matrix elements for the Hamiltonian of the AlSb layers in order to yield a valence band offset of 0.2 eV (top of valence band higher in AlSb).[22] The Hamiltonian matrix elements of the AlAs (InSb) interfacial layer was determined as follows: the intraorbital elements of the Al (Sb) and As (In) atoms were taken to be the same as for the corresponding atoms in the AlSb and in the InAs layers, respectively. The matrix elements between Al (In) and As (Sb) orbitals, on the other hand, were assumed to be equal to those in bulk AlAs (InSb).

The imaginary part of the dielectric function was calculated by integrating the matrix elements for optical transitions between the valence and conduction bands over the superlattice Brillouin zone using the tetrahedron method.[23–25] The optical transition elements were obtained directly from the tight-binding Hamiltonian using the procedure described in Refs. 24 and 25.

The tight-binding results for the optical anisotropy are summarized in Figs. 5(a)–5(c). Figure 5(a) displays the calculated difference in the imaginary part of ϵ along the [011] and [01$\bar{1}$] directions for a superlattice with InSb and AlAs interface bonds in the bottom and top interfaces of the InAs layers, respectively. In agreement with the experimental results, the anisotropy spectra are dominated by the structures near the E_1 critical points of the two materials. It is interesting to note that the E_1 contributions are of opposite signs for the InAs and for the AlSb layers. This behavior can be easily understood by assuming that the asymmetric interfaces introduce potential gradients along the [100] direction of magnitudes $\phi^{\rm InAs}(x)$ and $\phi^{\rm AlSb}(x)$ and of opposite orientations in the InAs and in the AlSb layers, respectively. If $\phi^{(i)}$ is small, an expansion of the dielectric constant yields

$$\epsilon^{(i)} = \epsilon^{(i)}_{ij} + \epsilon^{(i)}_{ijk}\phi^{(i)}_k + \epsilon^{(i)}_{ijkl}\phi^{(i)}_k\phi^{(i)}_l \ldots . \qquad (2)$$

For the D_{2d} point group the first and third terms at the right-hand side of Eq. (2) yield isotropic contributions to the dielectric function. Only ϵ_{ijk} with $i \neq j \neq k$ is nonzero in the second term, so that the anisotropy is given by

$$\epsilon_{[011]} - \epsilon_{[01\bar{1}]} = 2\epsilon^{\rm InAs}_{yzx}\phi^{\rm InAs} - 2\epsilon^{\rm AlSb}_{yzx}\phi^{\rm AlSb}. \qquad (3)$$

If the ϵ^i_{yzx} exhibit similar resonant behavior as the dielectric function the anisotropy spectra should contain contributions of opposite signs from the critical points of the InAs and of the AlSb layers, in agreement with the tight-binding and experimental results for samples with InSb interface bonds.

The effects of chemical mixing at the interfaces on the optical properties of the layers can also be estimated by the microscopic tight-binding calculations. Figure 5(b) displays the anisotropy in a superlattice with InSb interface bonds where 30% of the Sb atoms at the bottom interfaces of the InAs layers were exchanged by As. In agreement with the expected symmetry, calculations

yield no anisotropy in structures with only InSb interface bonds. The spectrum was calculated by using for the tight-binding parameters of the mixed interface a weighed average between those of InSb and of AlAs. Results for an interface where 30% of the In atoms have been substituted for Al is shown in Fig. 5(c). In both cases, the line shape is similar and the amplitude of the anisotropy is approximately 1/3 of that calculated for an ideal structure with alternating InSb and AlAs interfaces [Fig. 5(a)].

Figure 5(d) reproduces for comparison $\mathrm{Im}(\epsilon_{[011]} - \epsilon_{[01\bar{1}]})$ measured in superlattices with nominally only InSb interfaces. The magnitude of the measured anisotropy [Fig. 5(d)], of approximately 1 unit in the dielectric function, is comparable to that obtained from the calculations [Figs. 5(a)–5(c)]. The calculated spectra, however, do not reproduce all the features observed experimentally. The contribution around 3 eV of the critical point E_1 of the AlSb layers is overestimated in the calculations. The differences between the measured and calculated spectra are worse in the case of superlattices with AlAs interface. These differences arise in part due to the approximations used in the calculation (e.g., neglect of spin effects). In addition, interface mixing is only partially taken into account, since the superlattices with mixed interface bonds in the calculations are still periodic structures with full translational symmetry.

B. Disorder effects

In order to quantify the effects of disorder on interface asymmetry we will assume that for energies around the E_1 gap the optical properties are basically determined by the local composition. This assumption is partially justified by the fact that the energy location of the main features in the superlattice spectra (see, for instance, Fig. 3) are close to those in the corresponding bulk materials. In this approximation the dielectric constant of the superlattice can be calculated in the framework of the bond polarizability model as the sum of contributions from single bonds. For each bond we associate energy-dependent polarizabilities $\alpha_{\parallel}$ and $\alpha_{\perp}$ for electric fields parallel and perpendicular to the bond, respectively. For a bond oriented in the [111] direction (see Fig. 1) the difference in polarizability $\alpha^{[111]}_{[011]}$ and $\alpha^{[111]}_{[01\bar{1}]}$ for fields in the [011] and in the $[01\bar{1}]$ directions, respectively, is then given by the expression

$$f_\alpha^{[111]} = \frac{\alpha^{[111]}_{[011]} - \alpha^{[111]}_{[01\bar{1}]}}{\bar{\alpha}} = -\frac{2(\alpha_\perp - \alpha_\parallel)}{2\alpha_\perp + \alpha_\parallel} . \tag{4}$$

In this expression, the superscripts specify the bond direction and

$$\bar{\alpha} = \frac{2\alpha_\perp + \alpha_\parallel}{3} \tag{5}$$

is the polarizability averaged over all field directions. For a bond oriented in the $[11\bar{1}]$ the relative difference in polarizability becomes $f_\alpha^{[11\bar{1}]} = -f_\alpha^{[111]}$. The total polarizability in a given direction can then be obtained as a sum of the contributions of individual bonds.

The effects of the interfaces on the anisotropy can be readily calculated using the bond polarizability model described above. Structures with AlAs interface bonds will be considered first. If the bottom interface of the InAs layers is formed by AlAs bonds [see Fig. 1(a)], the exchange of an As atom by a Sb atom leads to the disappearance of two AlAs and two InAs bonds, and to the creation of two AlSb and two InSb bonds. The exchange introduces an anisotropy in the polarizability given by $\frac{\alpha_{[011]} - \alpha_{[01\bar{1}]}}{\bar{\alpha}} = 2\left[(f_\alpha^{\mathrm{InSb}} + f_\alpha^{\mathrm{AlAs}}) - (f_\alpha^{\mathrm{InAs}} + f_\alpha^{\mathrm{AlSb}})\right]$, where, for each bond type, $f_\alpha = -f_\alpha^{[111]}$. Note that the exchange of an atom As by Sb within a InAs layer (i.e., away from interfacial bilayer) does not introduce anisotropy since two InSb bonds are simultaneously introduced in the [011] and in the $[01\bar{1}]$ planes. The anisotropy, therefore, arises primarily from the differences in the interfacial composition and is less sensitive to material intermixing within the layers.

Since the dielectric function difference is proportional to the polarizability difference, the arguments of the previous paragraph can be extended to show that if fractions p_a^I and p_a^{II} (p_c^I and p_c^{II}) of the interface As (Al) atoms are substituted by Sb (In) at bottom and top interfaces of the InAs layers, respectively, the anisotropy in the dielectric function is given by

$$\epsilon_{[011]} - \epsilon_{[01\bar{1}]} = \frac{p}{2N}[(f_\alpha^{\mathrm{InSb}}\epsilon^{\mathrm{InSb}} + f_\alpha^{\mathrm{AlAs}}\epsilon^{\mathrm{AlAs}}) - (f_\alpha^{\mathrm{InAs}}\epsilon^{\mathrm{InAs}} + f_\alpha^{\mathrm{AlSb}}\epsilon^{\mathrm{AlSb}})] \tag{6}$$

where $p = (p_a^I - p_a^{II}) + (p_c^I - p_c^{II})$ is a parameter that quantifies the disorder and N is the number of bilayers in the superlattice period. A similar expression, but with opposite sign, applies to superlattices in InSb interface bonds.

Equation (6) shows that the anisotropy depends on the difference in the compositional disorder of the two interfaces. The maximum anisotropy occurs when one interface is perfect and all cations (or anions) in the other are interchanged. This situation is equivalent to that encountered in a periodic superlattice with alternating AlAs-like and InSb-like interfaces. A maximum in the anisotropy also occurs if both cations and anions are exchanged with 50% probability, so as to generate an interfacial layer with average composition $Al_{0.5}In_{0.5}Sb_{0.5}As_{0.5}$. Note, in addition, that from the sign of p which represents best the experimental data it is possible to determine which is the more disordered interface.

The imaginary part of the dielectric constant obtained from Eq. (6) is displayed by the circles in Figs. 4(a) and 4(b) for structures with AlAs and InSb interface bonds, respectively. Two assumptions were made in the calculation. First, we assumed that $f_\alpha = 1$ for all materials. This assumption is probably valid near the E_1 gap of the bulk materials, where the dielectric function is dominated by the contribution of the bands at the Λ lines ($\langle 111\rangle$ directions) and one expects $\alpha_\perp \gg \alpha_\parallel$. Second,

the bond polarizabilities were assumed to be the same as in the corresponding bulk materials. This assumption is certainly not strictly valid close to the interfaces where the environment of the bonds differs appreciably from the bulk case. Note that in this approximation Eq. (4) predicts similar anisotropies for samples with AlAs and with InSb interface bonds.

The disorder parameter p does not affect the energy dependence of the anisotropy and was adjusted to give the best possible agreement with the experimental data. The circles in Figs. 4(a) and 4(b) were calculated using $p = 0.4$ and $p = -0.4$, respectively. For superlattices with AlAs interface bonds Eq. (4) reproduces surprisingly well the measured anisotropy, especially if we take into account the simplicity of the model used. The sign of p indicates that the bottom interfaces of the InAs layers are considerably more disordered than the top interfaces, with approximately 40% of the interface atoms being exchanged. This result is in agreement with the previously reported lower quality of the bottom AlAs-like interface of AlSb/InSb/AlSb quantum wells.[5]

The large degree of interface disorder in superlattices with AlAs interface bonds is in agreement with previous x-ray, transport, and Raman investigations on similar structures.[5–7,26] It was found that in contrast to structures with InSb interfacial bonds, superlattices with AlAs interface bonds exhibit larger lattice relaxation and a considerable amount of As in the AlSb layers. In fact, the As concentration determined from the Raman shift of the AlSb phonons corresponds to the presence of a two-monolayer thick $AlSb_{0.5}As_{0.5}$ interface alloy,[6,7] in quantitative agreement with the degree of disorder determined from the RDS measurements. Note, however, that if the anisotropy is produced by As contamination of the AlSb layer, the data presented here indicate that this contamination takes place when the AlSb layers are exposed to the interfacial As flux.

Equation (4) predicts the same spectral dependence of the anisotropy for superlattices with AlAs and InSb interface bonds and does not reproduce the structures between 3 and 4 eV in superlattices with InSb interface bonds [see Fig. 4(b)]. We conclude, therefore, that disorder effects are not the dominant ones in these structures.

The bond polarizability model provides an intuitive way of understanding the dependence of the anisotropy in the superlattices where the bottom interfaces of the InAs layers are formed by AlAs bonds [Figs. 2(c) and 2(d)]. If interfaces with AlAs bonds are more disordered than those with InSb bonds, the difference in degree of disorder and, therefore, the anisotropy should increase when the top interfaces of the InAs layers are changed from AlAs to InSb, in agreement with the results in Figs. 2(c) and 2(d).

Finally, since each interface in an InAs/AlSb superlattice has individually a C_{2v} symmetry, one may expect a contribution to the anisotropy arising from the strong absorption of the incoming light. We estimated the absorption contribution using the bond polarizability model and assuming that the contribution of each bond to the dielectric function is proportional to the light intensity at the bond location. The absorption coefficient of the superlattice was estimated from the measured values of the bulk layer materials.[28] We found the absorption contribution to be a factor of at least ~ 5 smaller than the measured anisotropy.

C. Interface roughness

In this section we estimate the contribution to optical anisotropy from interface roughness caused by lateral variations in layer thickness. As mentioned before, the layer thickness variations must be oriented along one of the main optical axes of the superlattices ([011] or [01$\bar{1}$]) in order to yield an anisotropic contribution to the optical properties. If the length scale of the roughness is small compared to the light wavelength used in the RDS experiments, the anisotropy can be estimated using an effective medium approximation for the optical properties. We shall assume that the roughness is oriented in the **a** direction (either [011] or [01$\bar{1}$]) along the surface (i.e., the layer thickness is constant perpendicular to the **a** direction) and has an average amplitude δ. The dielectric constant for the electric field perpendicular and parallel to the **a** direction can then be obtained by averaging the contributions ϵ^i and $1/\epsilon^i$, respectively, of the different layers,[27]

$$\epsilon_{\mathbf{a}} - \epsilon_{\mathbf{b}} \sim -\frac{\delta}{d}\frac{(\epsilon^{\mathrm{InAs}} - \epsilon^{\mathrm{AlSb}})^2}{\epsilon^{\mathrm{InAs}} + \epsilon^{\mathrm{AlSb}}}, \tag{7}$$

where d is the superlattice period, **b** is the surface direction perpendicular to **a**, and ϵ^i is the dielectric constant of the ith layer (assumed to be equal to the bulk value).

The circles in Fig. 6 show the anisotropy calculated from Eq. (7) for $\delta/d = 0.1$ and **a** along [01$\bar{1}$], together with the anisotropy spectrum for a superlattice with InSb interface bonds. In these superlattices, the optical anisotropy in the energy range from 1.5 to 3 eV

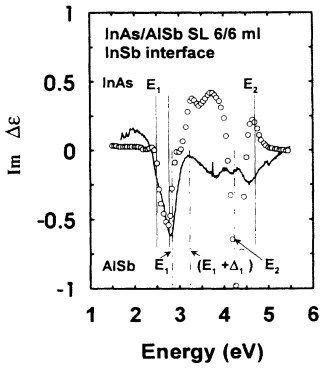

FIG. 6. Imaginary part of the difference $\Delta\epsilon = \epsilon_{[011]} - \epsilon_{[01\bar{1}]}$ in the dielectric constant in the [011] and in the [01$\bar{1}$] directions for InAs/AlSb superlattices with InSb interface bonds (thick line). The circles display the anisotropy expected from an oriented interface roughness equal to 10% of the superlattice period (see text for details). The vertical solid and dot-dashed lines show the energy position of the critical points for bulk InAs and AlSb, respectively.

is well reproduced by the interface roughness model if one assumes a thickness fluctuation of approximately one bilayer. This good agreement indicates that the roughness mechanism is probably the dominant one in superlattices with InSb interface bonds. A similar roughness amplitude was obtained from the dependence of the electron mobility on the InAs layer thickness in superlattices with InSb interface bonds,[29] further supporting the interface roughness anisotropy mechanism.

The roughness model fails to reproduce the features observed for larger photon energies, especially those near the E_2 gaps. This is probably due to the fact that the light penetration depth is comparable to the superlattice layer thickness, so that the simple model developed here is no longer valid. Finally, since the spectral dependence of the roughness-induced anisotropy is in a first approximation independent of the interface type, a similar spectral form is expected for superlattices with AlAs interfaces. We conclude, therefore, that the roughness mechanism plays a secondary role in these superlattices since a different line shape is observed [see Fig. 4(a)].

V. CONCLUSIONS

We have investigated the optical anisotropy of InAs/AlSb superlattices with different types of interface bonds. Superlattices with a single type of interface bond (InSb or AlAs) are expected to be optically isotropic in the plane of the layers. Contrary to this expectation, the reflection coefficient differs by $\sim 2\%$ for incident light polarizations in the [011] and in the [01$\bar{1}$] directions. The anisotropy changes with interface composition, indicating that it is interface related. Different mechanisms for the anisotropy were investigated. In superlattices with AlAs interface bonds the anisotropy originates in the disordered material near the interfaces. It arises from differences in the degree of chemical disorder between the interfaces where InAs is grown on AlSb and the ones where AlSb is grown on InAs. Chemical disorder leads to the creation of InSb bonds in the case where nominally only AlAs bonds should be present. The InSb bond density was found to be approximately 30%–40% larger at the bottom than at the top interfaces of the InAs layers.

The origin of the anisotropy in superlattices with nominally only InSb interfaces is less clear. Although the anisotropy still should be related to the composition of the interface, the disorder mechanism mentioned above seems to play a secondary role in these structures. Two possible anisotropy mechanisms are (i) the presence of oriented interfacial roughness and (ii) the existence of potential fields across the layers induced by differences in between the bottom and top interfaces of each layer. Although a clear distinction between the two mechanisms is difficult since they yield contributions to the anisotropy of similar spectral shape, the better agreement with the experimental results suggests that the roughness mechanism is the dominant one.

ACKNOWLEDGMENT

We thank M. Kuball for discussions and for a critical reading of the manuscript.

[1] H.W. van Kesteren, E.C. Cosman, W.A.J.A. van der Poel, and C.T. Foxon, Phys. Rev. B **41**, 5283 (1990).
[2] P. Lavallard, C. Gourdon, and R. Planel, Superlatt. Microstruct. **12**, 321, 1992.
[3] I.L. Aleiner and E.L. Ivchenko, Pis'ma Zh. Eksp. Teor. Fiz. **55**, 662 (1992) [JETP Lett. **55**, 692 (1992)].
[4] P.M. Young and H. Ehrenreich, Appl. Phys. Lett. **61**, 1069 (1992).
[5] G. Tuttle, H. Kroemer, and J. English, J. Appl. Phys. **67**, 3032 (1990).
[6] J. Spitzer, H.D. Fuchs, P. Etchegoin, M. Ilg, M. Cardona, B. Brar, and H. Kroemer, Appl. Phys. Lett. **62**, 2274 (1993).
[7] J. Spitzer, H.D. Fuchs, P. Etchegoin, A. Höpner, M. Ilg, M. Cardona, B. Brar, and H. Kroemer, *Proceedings of the 4th Internatioinal Conference on the Formation of Semiconductor Interfaces, Jülich, Germany, 1993* (World Scientific, Singapore, in press).
[8] J. Spitzer, A. Höpner, M. Kuball, M. Cardona, B. Jenichen, H. Neuroth, B. Brar, and H. Kroemer (unpublished).
[9] D.E. Aspnes, J. Vac. Sci. Technol. B **3**, 1498 (1985).
[10] D.E. Aspnes, J.P. Harbison, A.A. Studna, and L.T. Flores, J. Vac. Sci. Technol. **A** 6, 1327 (1988).
[11] O. Acher and B. Drévillon, Rev. Sci. Instrum. **63**, 5332 (1992).
[12] *Semiconductors: Physics of Group IV Elements and III-V Compounds*, edited by O. Madelung, Landolt-Börnstein, New Series, Vol. 17, Pt. a (Springer-Verlag, Heidelberg, 1982).
[13] S. Zollner, Ph.D. thesis, University of Stuttgart, 1991.
[14] M. Garriga, PhD. thesis, University of Stuttgart, 1990.
[15] D.E.Aspnes and A.A. Studna, Phys. Rev. Lett. **54**, 1956 (1985).
[16] S. Selci, F. Ciccato, G. Chiarotti, P. Chiaradia, and A. Cricenti, J. Vac. Sci. Technol. **A** 5, 327 (1987).
[17] S.E. Acosta-Ortiz and A. Lastras-Martinez, Solid State Commun. **64**, 809 (1987).
[18] W. Luis Mochán and R.G. Barrera, Phys. Rev. Lett. **55**, 1192 (1985).
[19] J.H. Neave, B.A. Joyce, P.J. Dobson, and N. Norton, Appl. Phys. A31, 1 (1983).
[20] M. Tanaka, H. Sakaki, and J. Yoshino, Jpn. J. Appl. Phys. **25** L155 (1986).
[21] P. Vogt, H. Hjalmarson, and J. Dow, J. Phys. Chem. Solids **44**, 365 (1983).
[22] The measured valence band offset in InAs/AlSb interfaces lies between 0.15 and 0.22 eV, see J.R. Waldrop, G.J. Sullivan, R.W. Grandt, E.A. Kraut, and W.A. Harrison, J. Vac. Sci. Technol. B **10**, 1773 (1992).
[23] O. Jepsen and O. K. Andersen, Solid State Commun. **9**, 1763 (1971); G. Lehman and M. Taut, Phys. Status Solidi B **54**, 469 (1972).
[24] G. Dresselhaus and M.S. Dresselhaus, Phys. Rev. **160**, 649 (1967).

[25] L.C. Lew Yan Voon and L.R. Ram-Mohan, Phys. Rev. B **47**, 15 500 (1993).
[26] I. Sela, C.R. Bolognesi, L.A. Samoska, and H. Kroemer, Appl. Phys. Lett. **60**, 3283 (1992).
[27] D.E. Aspnes, J. Opt. Soc. Am. **63**, 1380 (1973).
[28] D.E. Aspnes and A.A. Studna, Phys. Rev. B **27**, 985 (1983).
[29] C.R. Bolognesi, H. Kroemer, and J.H. English, Appl. Phys. Lett. **61**, 213 (1992); J. Vac. Sci. Technol. B **10**, 877 (1992).